

Real-time Simulations on High-Performance Z-Source PV-Grid-Tied Inverters with DC Charger for EV Applications

D SHEKSHAVALI

ASSISTANT PROFESSOR

shaiksha456@gmail.com

A RAMESH

ASSISTANT PROFESSOR

ramesh.andhala@gmail.com

G MADHU

ASSISTANT PROFESSOR

Department of Electrical and Electronics Engineering Sri Venkateswara Institute of Technology, N.H 44, Hampapuram, Rappthadu, Anantapuramu, Andhra Pradesh 515722

Abstract

Solar power has emerged as the go-to renewable energy option for homes and light businesses. Energy storage devices (ESS) may make solar power harvesting more stable by reducing the impact of environmental factors. Using solar energy to charge EV batteries is another way to reduce grid dependency. These converters meet certain requirements, one of which being a separation feature and a small number of conversion steps. The elimination of unnecessary steps and

the consolidation of dc-to-ac power conversion into a single stage are both made possible by the Z-source inverter (ZSI) architecture. Integrating energy storage systems (ESS) with passive materials becomes possible when they are used. For direct current (dc) charging of EV battery packs, this article details the modelling, building, and functioning of an altered ZSI coupled with a split primary separated battery charger. We have provided simulation results as proof of concept for the functioning of the proposed converter.

Keywords: SRM, Inverter, EV, speed, load.

1. Introduction

Currently, an alternating current (AC) grid is used extensively for the charging of electric vehicles (EVs). No matter how efficient the topology is, certain charging techniques that rely only on the AC grid—like wireless charging or plug-in charging—can nevertheless lead to pollution. The carbon footprint left behind after charging an electric vehicle may be better understood by looking at the quantity of fossil fuels used to produce the electricity. Integrating renewable

energy sources into a charging infrastructure to decrease reliance on the electrical grid is one strategy to attain reduced carbon footprints [1]. Isolation transformers are an essential component in electric vehicle (EV) battery charger designs, as they isolate the user's end of the system from the rest of the high-voltage system and offer galvanic isolation. Either the AC grid or the charger may provide the galvanic isolation [2]. It is common practice for the isolation transformer

on the grid side to be much bigger than its charger side counterpart. Now that semiconductor technology has advanced, smaller transformers may be used for galvanic isolation thanks to high-frequency switching [3]. In the past, commercial charging infrastructure has made use of photovoltaic (PV) grid linked systems. The charging infrastructure's reliance on the ac grid is reduced by these solutions. One promising option for home EV charging systems is the integration of solar power with grid-connected systems [4]. Residential applications may use systems with single-phase inverters up to 10 kW. There are a number of different multi-stage isolated and non-isolated topologies that may be used to link home solar PV to the grid. Isolation and voltage boost capabilities are two elements that residential PV systems

for EV charging must have in order to match the voltage of the solar PV array to the grid voltage requirements [5]. It can flip the input dc voltage in a single step and buck or boost it as well. In PV-grid-connected applications, it has become quite popular. The Z-Source Multiplier

Two inductors and two capacitors make up the (ZSI) topology, which is used to increase the input dc voltage until it meets the requirements of the inverter-side ac output voltage. The passive parts of a ZSI are crucial to its functioning [6]. The chance to include energy storage units into that kind of system is presented by it. This project showcases an application towards a string inverter arrangement using a solar grid-connected charger based on a single-phase Modified Z-source Inverter (MZSI).

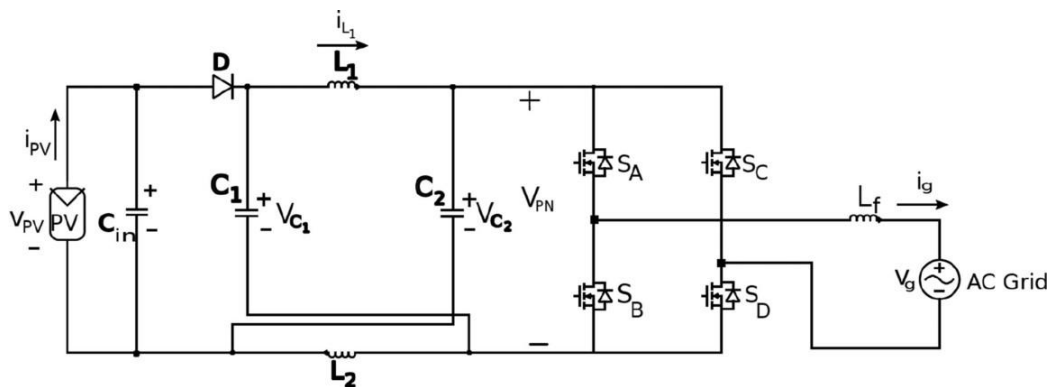


Figure1. Schematic of a PV/ac Grid Interconnected ZSI

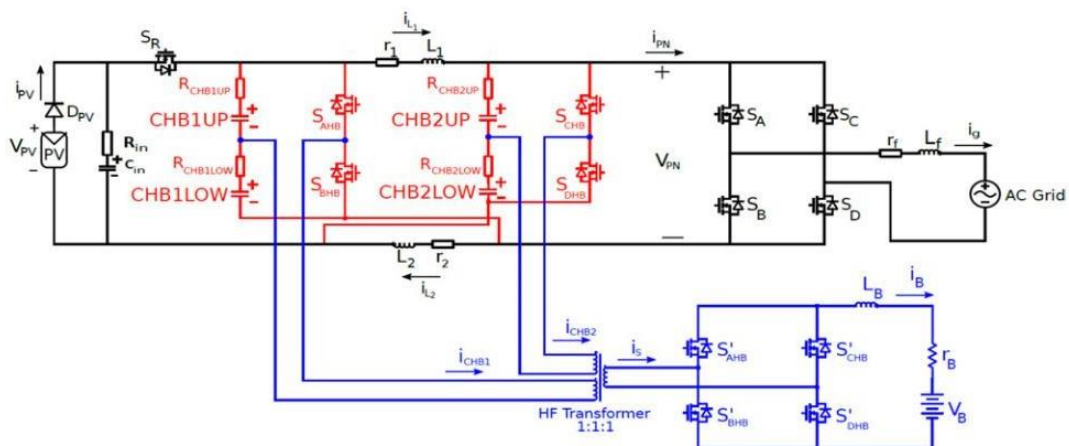


Figure2. Detailed Schematic of the Proposed MZSI

1.2 Literature Survey

This research focuses emphasis on recently created PE infrastructure technologies that allow for rapid battery charging procedures, including those mentioned by D. Aggeler et al. [7]. These days, Power Electronics (PE) is making inroads into technologies that were formerly considered to be part of other branches of engineering. One such example is e-mobility. As a new field that aims to improve sustainable mobility, power electronics is already making waves in the engineering world. It covers everything from energy distribution for charging to energy transformation in traction-related vehicles. Recharging a battery to the point where it can cover over 100 km in under 10 minutes is possible with most vehicles and types of batteries [8]. Recharging will soon be as easy as stopping at a petrol station, thanks to the ever-improving technology behind batteries. In this presentation, we will examine two PE converter designs for infrastructure charging applications, one for low-frequency (LF) isolation and one for high-frequency (HF) isolation. We will discuss and provide a technical review of the two technologies, including their advantages and disadvantages. Under the premise of a DC fast charging station situated in a rural region of Sweden, the effects on the grid are investigated by computational modelling. The study by G. Carli and S. S. Williamson [9] examines the charging needs of electric vehicles through the lens of a particular kind of renewable energy: local energy production. It is already obvious that power and the associated infrastructure required for storage and distribution will play an increasingly important role in the transportation industry.

Simultaneously, the power source itself cannot contain carbon. Instead, it needs to rely on eco-friendly procedures wherever feasible. In addition to being good for the environment, aeolic and photovoltaic (PV) sources may be used for local production and delivery, cutting down the energy losses that come with distributing power over vast distances on the grid. The PV source is specifically mentioned since solar panels may be positioned over the parking spot and also serve to offer shade. The ideal system requirements are determined in the first section of this article. Part 2 will make use of them to evaluate and contrast various power conditioning circuits for this purpose.

In order to determine whether the current power system's capacity is sufficient to handle the load demand from plug-in hybrid electric vehicles (PHEVs), a discrete-event simulation framework was developed. This framework was described by S. Bai, D. Yu, and S. Lukic [10]. From actual statistical transportation data, we derive the probability distribution functions for each vehicle's arrival time and energy usage. The main limitations are thought to be the electricity grid's restricted transmission and generating capacity. That being said, cars may not get any charges right away. Applying the suggested modelling framework to two real-world examples in the US helps to justify and illustrate it in some depth, allowing one to identify which areas' grid potential may support PHEVs. Level -2 and Level 1 charges are also taken into account.

1.3 Problem Formulation

In order for the ac output voltage to be below or equal to the dc-rail voltage, or vice versa, the dc-rail voltage must be higher than the ac input voltage. It follows that the voltage source converter is a boost rectifier (or boost converter) for converting ac to dc power and the voltage source inverter is a buck (stepdown) inverter for converting dc to ac. An extra dc-dc boost converter is required to provide the appropriate ac output in cases where overdrive is desired but the available dc voltage is restricted. The efficiency and cost of the system are both negatively impacted by the extra power converter step. Whether intentional or caused by electromagnetic interference (EMI), the upper and lower devices of each phase leg cannot be gated on at the same time. In any other case, the gadgets would be destroyed in a shoot-through. A key threat to the converter's dependability is the shootthrough issue caused by misgating-on electromagnetic interference (EMI) noise. There is distortion in the waveform, etc., since the voltage source converter needs to account for dead time to block both the higher and lower devices. In contrast to the current-source inverter, an output LC filter is required to provide a sinusoidal voltage; this adds control complexity and power loss. For the dc inductor to function, the ac output voltage must be higher than the dc input voltage, or else the dc voltage output would always be lower than the ac input voltage. As a result, a buck rectifier (or converter) is used in the current source inverter

to convert alternating current (ac) to direct current (dc), and a boost inverter is used in the current source converter to convert dc to alternating current (ac). An extra dc-dc buck (or boost) converter is required for uses that benefit from a broad voltage range. The system's efficiency drops and its cost rises due to the extra power conversion step. To prevent reverse voltage from reaching the current source converter's primary switches, a series diode and high-speed, high-performance transistors such as insulated gate bipolar transistors (IGBTs) are used. Smart power modules (IPMs) and inexpensive IGBT modules with good performance can't be used directly because of this.

This paper introduces an impedance-source power converter, also known as an impedance-fed converter, and its control method for dc-to-ac, ac-to-dc, ac-to-ac, and dc-to-dc power conversion. Its purpose is to address the aforementioned issues with traditional voltage source and current source converters.

2. Formatting your Paper

Solar photovoltaic cells are basic p-n junction diodes that transform sunlight into usable power. In Figure 3, we can see a simplified schematic of a PV cell's equivalent circuit. A PV cell's output current is represented by the current source in this model. The model also includes a diode connected in parallel with the current source, a shunt resistance, and a series resistance.

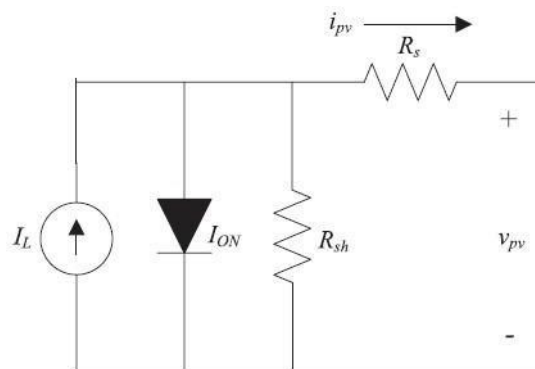


Figure 3 Equivalent circuit diagram of the PV cell

3. DC-DC Converters

A high-step-up DC-DC converter has several potential uses, including lighting systems for vehicles, systems that convert energy from fuel cells or solar panels, and systems that provide backup power from batteries for uninterruptible power sources. A high effective duty ratio should allow a dc-dc boost converter to achieve a high step-up voltage, at least in theory. To be more specific, power switches and the ESR of inductors and capacitors limit the step-up voltage gain in practice. To achieve a high step-up voltage gain and a big duty ratio, a traditional boost converter is often used. However, power switch and diode losses, inductors' and capacitors' equivalent series resistance, and diodes' reverse recovery difficulty limit efficiency and voltage gain. The converters' active switch causes power dissipation, high voltage stress, and transformer leakage inductance. An active switch may be protected against voltage spikes by using a resistor-capacitor-diode snubbed. However, the effectiveness is reduced as a consequence of them. Converters that have a low input ripple current are created using the linked inductor. By including an extra LC circuit with a linked inductor, these converters achieve very low input current ripple.

4. Inverter

The inverter is a piece of electrical equipment that changes the voltage and frequency of alternating current (AC) from direct current (DC) using the right transformers, switches, and control circuits. Static inverters are used in many applications due to their lack of moving components. They may be found in anything from tiny switching power supply found in computers to massive electric utility applications that transfer bulk power via high voltage direct current. It is usual practice to use inverters when converting DC power sources, such solar panels or batteries, into AC electricity. An electronic oscillator with a high output power is what the electrical inverter is. The term "inverted" comes from the fact that the first mechanical AC to DC converters changed the direction of current flow from DC to AC by turning the machine backwards.

4.1 Cascaded H-Bridges Inverter

As seen in Figure 4, an m-level cascaded inverter has a single phase construction.

A single phase full bridge inverter, often known as an H-bridge, is linked to each

individual DC source, or SDCS. Simply by rearranging the four switches—S1, S2, S3, and S4—from the DC source to the dc/ac output, each inverter level may produce one of three voltage outputs: +V, 0, or -V. Turning on switches S1 and S3 will produce -Vdc, whereas turning on switches S1 and S4 will produce +Vdc. The output voltage is set to zero by activating either S1 and S2 or S3 and S4. The voltage waveform that is synthesised is equal to the sum of the

inverter outputs, which are the AC outputs of the various full bridge inverter levels. For a cascade inverter, the number of output phase voltage levels, denoted as m, is equal to 2s+1, where s is the number of independent DC sources. Figure 5 shows the phase voltage waveform of an 11-level cascaded H-bridge inverter with 5 complete bridges and 5 solid-state rectifiers. The voltage at the phase

$$v_{a1} + v_{a2} + v_{a3} + v_{a4} + \dots (1)$$

For stepped waveforms such as the one depicted in Figure 5 with s steps, the Fourier Transform for this waveform follows

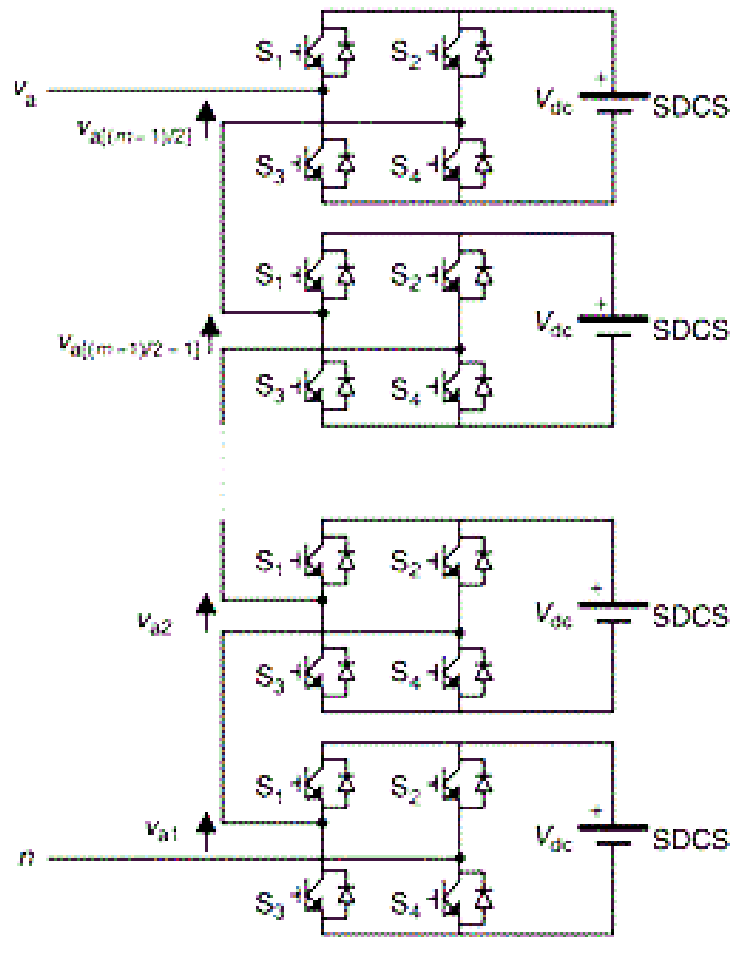


Figure 4. Single-phase structure of a multilevel cascaded H-bridge inverter

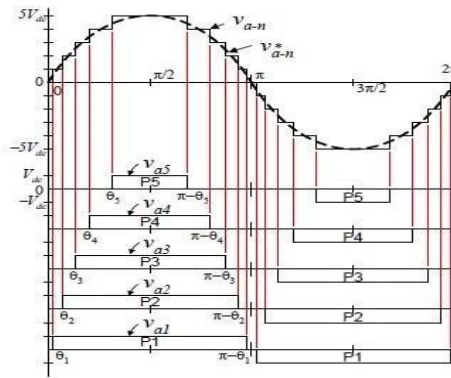


Figure 5 Output phase voltage waveform of an 11 level cascade inverter with 5 separate dc sources

5. Project Description and Control Design

5.1 Traditional ZSI

The ZSI topology, shown in Figure 7, utilizes two modes of operation: the shoot-through state and the non-shoot-through state. For symmetrical operations, we have

$$V_C = V_{C1} = V_{C2} \dots (2)$$

In the shoot-through state, all four switches

S_A, S_B, S_C and S_D , are conducting at the same time. The duration of this shoot-through state is described by the duty cycle D_0 and the switching frequency (F_{sw}). The shoot-through state can be implemented by a modified pulse width modulation (PWM) technique. Therefore, the two capacitor voltages are expressed as

$$V_C = (1 - D_0) / (1 - 2D_0) V_{pv} \dots (3)$$

The peak dc-link voltage V_{PN} is given by

$$V_{PN} = 1 / (1 - 2D_0) V_{pv} \dots (4)$$

The power balance equation between the dc and ac sides of the ZSI is expressed as

$$(1 - D_0) V_{PN} I_{PN} = I_{grms} V_{grms} \dots (5)$$

Where I_{PN} and V_{PN} are the peak dc-link current and voltage, respectively. The peak ac voltage of the ZSI is

$$V_g = M V_{PN} \dots (6)$$

Where M is the modulation index, the grid voltage v_g

$= V_g \sin \omega t$, and the grid current $i_g = I_g \sin(\omega t + \phi)$ for $\phi = 0$ for grid-connected applications. From (11) and (13), the RMS of the output ac voltage of the ZSI is

$$V_{grms} = M V_{pv} / (\sqrt{2} (1 - 2D_0)) \dots (7)$$

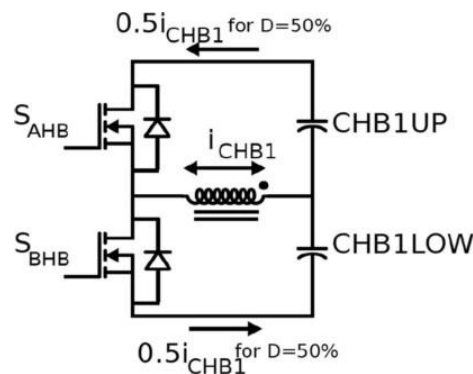


Figure 6. Schematic of one of the primary ac cross CHB1 operating at 50% duty cycle

5.2 Component Sizing, Modeling, and Control of the Proposed MZSI

A suggested MZSI with an integrated charger is shown in Figure 7. As shown in Figure 6, the two capacitors C1 and C2 are divided in half. When necessary, each half serves as a primary in the split primary isolated half-bridge bidirectional operation of the MZSI. In order to prevent electricity from flowing back into the PV, the diode DPV is used. The input capacitor Cin's internal resistance is Rin. The charger side of the MZSI may be integrated with a split primary isolated dc-to-dc converter for symmetrical operation. A high-frequency transformer separates the two HBC primary that make up the split primaries from one complete bridge secondary. In an open loop, the HBC primary and secondary are run at 50% duty cycle. A lithium-ion battery or other energy storage device receives the secondary's output current. By clamping its own voltage vB across the HBC primary' input VC, the energy storage unit charges the battery while the split primaries run in a clockwise fashion, supplying half of the battery's current demand. The capacitors on each side of the dc-dc converter link the two primary. When applied across capacitors, the voltage is given by (15). Figure 7 shows the simple equivalent model, which may be used to represent the two primaries, by connecting an RLE circuit in parallel to capacitors C1 and C2. Figure 7 shows the same diagram of the MZSI model in its non-shoot-through condition, where the KVL equation is $L \frac{di_L}{dt} = v_{pv} - i_L r + R_{HB} + (2i_g + i_B/2) R_{HB} - V_C$ (12) The Kirchoff's current law (KCL) equation is

$$C \frac{dV_C}{dt} = i_L - i_g - i_B/4 \quad \dots\dots(13)$$

During the shoot-through state, the KVL equation is

$$L \frac{di_L}{dt} = V_C - i_L (R_{HB} + r) - (i_B/2) R_{HB} \quad \dots\dots(14)$$

The KCL equation is written as

$$C \frac{dV_C}{dt} = -i_L - i_B/4 \quad \dots\dots(15)$$

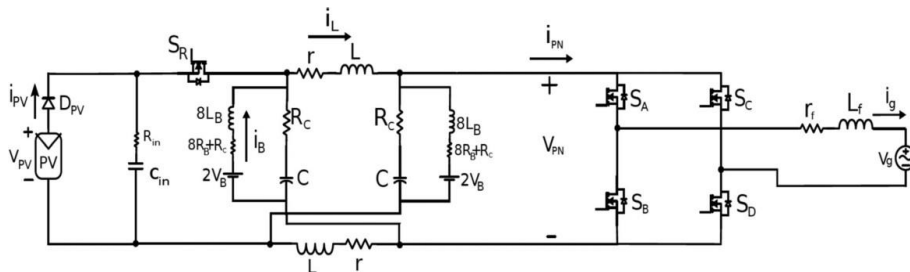
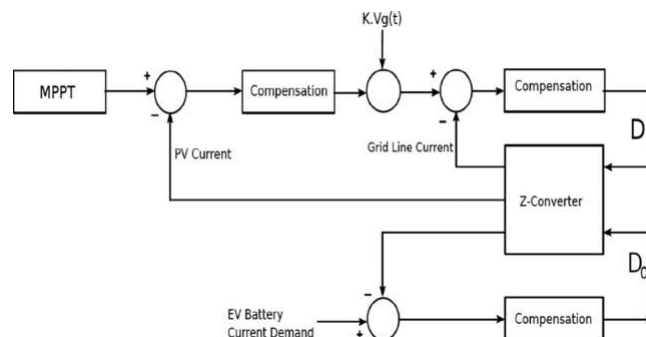


Figure 7. Equivalent model of the proposed MZSI with a battery



topology is shown in Figure 8. It has three stages: the photovoltaic (PV) current loop, the grid current (ig), and the battery current (iB). The voltage of the ZSI capacitor is modulated in order to provide the shoot-through duty ratio D0 or the reference current for the H-bridge

charger

The positive directions of the grid-side ac current (ig) and the battery current (iB) are shown in Figure 7. The controller block design for the proposed MZSI

inverter output current. The peak input PV current is controlled in order to create the reference current. The shoot-through duty ratio D_0 is a function of voltage V_C , which may be applied across either capacitor or both. Battery loop control has the slowest reaction time when compared to input current control since it does not need quick dynamic adjustments. In order to regulate the battery loop.

5.3 Energy Management Scheme for the Proposed Converter

Figure 8. Shows a simplified block diagram of the proposed system. When an energy storage system (ESS) is integrated into a ZSI, (5) is modified as follows

$$V_P V_i PV = V_b i_b + i_{grms} v_{grms} \tag{18}$$

where i_b and v_b are the battery current and voltage, respectively. Figure 7 shows that the single-phase ac grid power P_g balances the power fluctuation of the PV source P_{pv} ; thus, a constant charge power P_B is obtained at the ESS. For EV battery charging using both the single-phase ac grid

and the PV power, the direction of the ac grid current i_g changes to negative while drawing power from the grid. The inverter side can be operated bidirectionally, and the PV and the grid provide power for the charger, maintaining the power balance

$$V_P V_i PV + i_{grms} v_{grms} = V_b i_b \tag{19}$$

As long as the voltage across the input capacitor C_{in} is maintained to at least the minimum value of the PV voltage, the MZSI can be operated as a grid-connected rectifier/charger in the absence of the PV.

6. Simulation Results

The simulation studies to demonstrate the behavior of the proposed topology have been carried out using PLECS 4 for a 3.3 kW charger for a string inverter configuration. Simulation has been carried out for the system shown in Figure 9 shows that at a simulation time $t = 1.75$ s, the input PV power reduces from 2.8 to 2 kW and the grid power increases from 710 to 1500 W to maintain the output charger power to 3.3 kW.

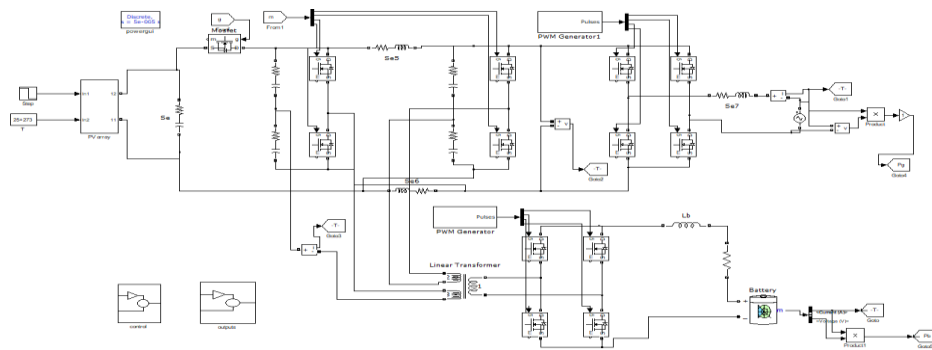


Figure 9. Overall Simulink diagram

Table 1. MZSI-Based Charger System Simulation Specifications

S.No	Parameters Value	Value
1	Input voltage, V_{in}	286 V
2	Input current, I_{in}	9.8A
3	Inductor value, $L_1=L_2$	500 μ H

4	ZSI switching frequency, FSW	25kHz
5	Grid voltage (RMS), V_g	240 V
6	Inverter output filter inductor, L_f	7.5mH
7	PV input power, PPV	2.8kW
8	Input capacitor, C_{in}	2mF
9	HBC output filter, LB	1mH
10	HBC output filter, LB	1mH
11	Battery charge power, PB	3.3kW

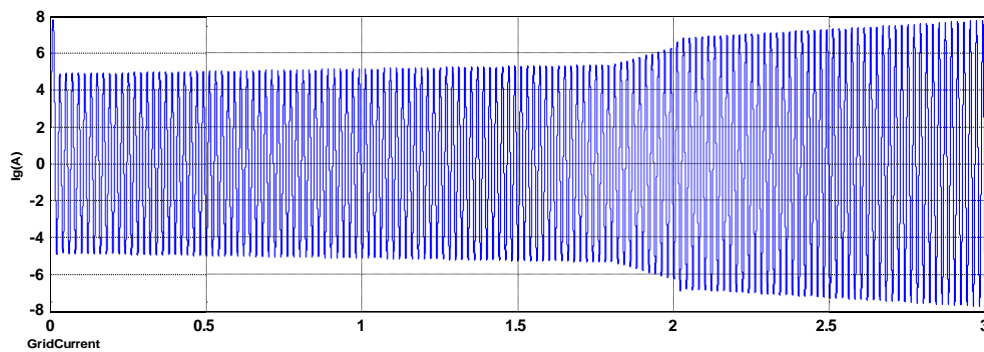


Figure 10. Output waveform of Grid current

The above figure shows the output waveform of grid current. In this X-axis represents time in seconds and Y-axis represents grid current in amperes.

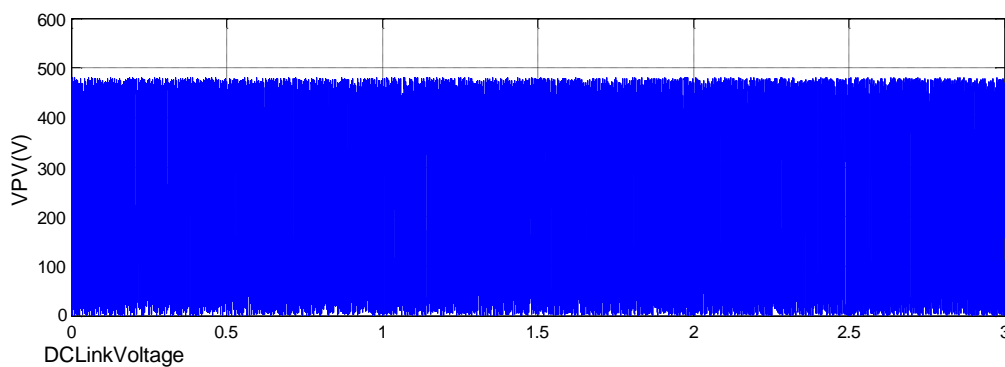


Figure 11. Output waveform of DC link voltage

The above figure shows output waveform of DC link voltage. In this X-axis represents time in seconds and Y-axis represents DC link voltage in volts.

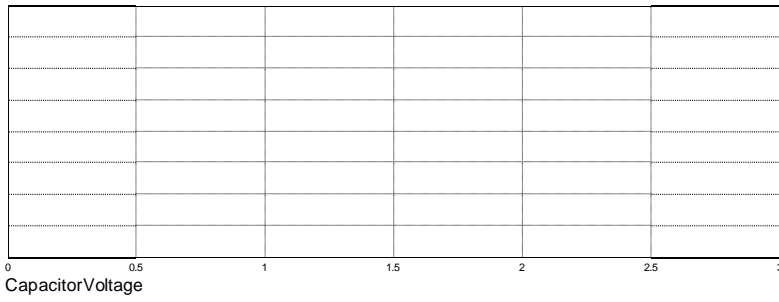


Figure 12. Output waveform of capacitor current

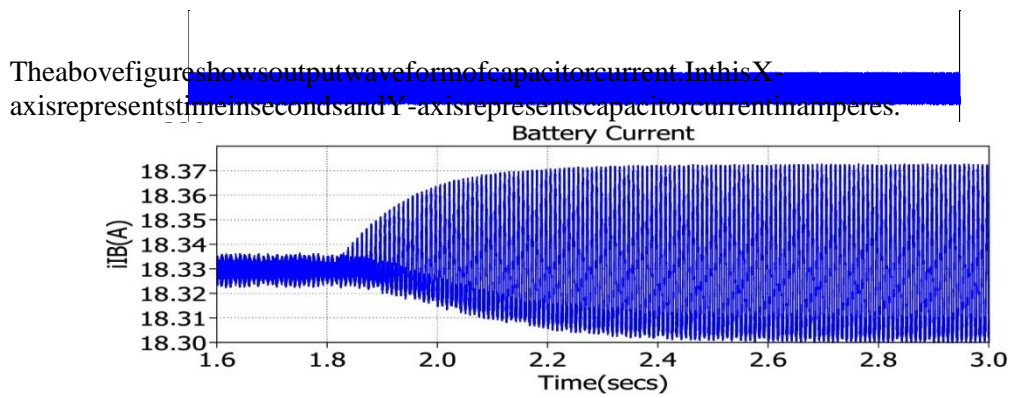


Figure13. Output waveform of battery current

The above figure shows output waveform of battery current. In this X-axis represents time in seconds and Y-axis represents battery current in amperes.

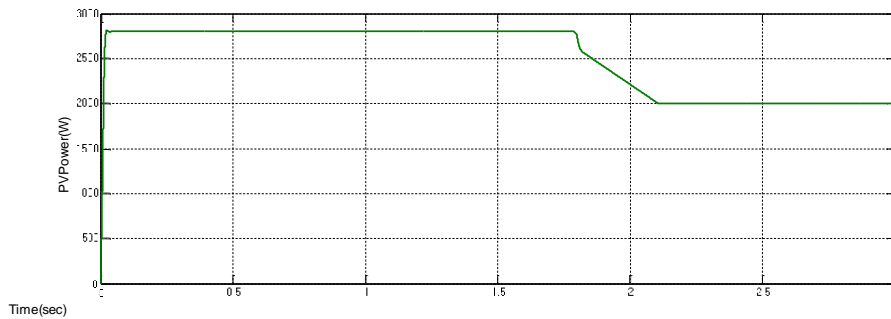


Figure14. Output waveform PV power

The above figure shows output waveform of PV power. In this X-axis represents time in seconds and Y-axis represents power in watts.

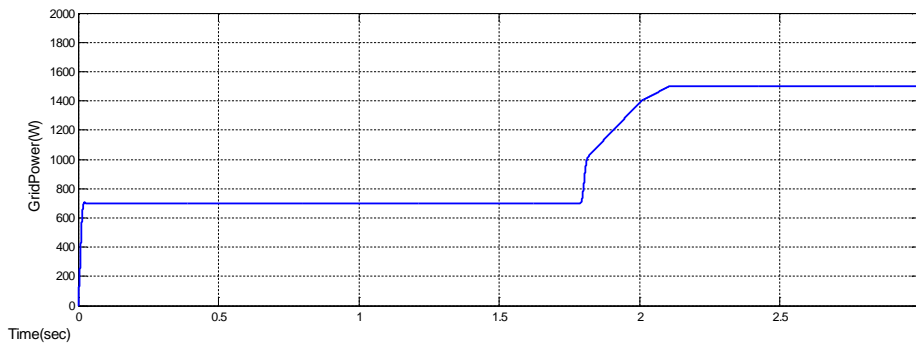


Figure15. Output waveform of Grid Power

The above figure shows output waveform of grid power. In this X-axis represents time in seconds and Y-axis represents grid power in watts.

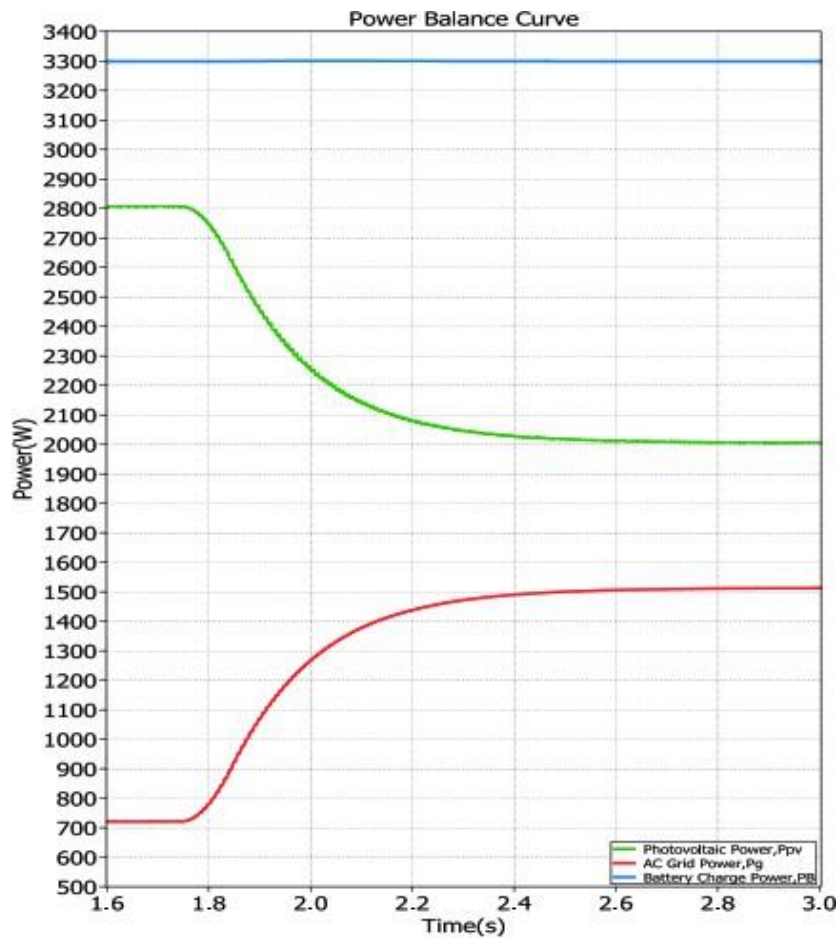


Figure16. Simulation waveform for the power balance between the PV input power, the ac grid side, and the battery power

Conclusion

An alternative to PV-grid-connected charging systems is proposed in this study, the MZSI architecture. A PV-grid connection with one stage and an integrated charger for charging or energy storage via the PV-grid are its main components. Clustered charging configurations using this topology are well-suited to semi-commercial spaces,

including parking lots of shopping malls. Applying this principle to home string inverter setups—with the charger side connected in series or parallel to share current—is a viable option. The symmetrical functioning of the impedance network of a Z-source converter was the basis for the energy storage design proposed in this research.

REFERENCES

Aggeler, D., Canales, F., Zelaya-DeLaParra, H., Coccia, A., Butcher, N., & Apeldoorn, O. (2010, October). Ultra-fast DC-charge infrastructures for EV-mobility and future smart grids. In 2010 IEEE PES Innovative Smart Grid Technologies Conference Europe (ISGT Europe) (pp. 1-8). IEEE.

Carli, G., & Williamson, S. S. (2013). Technical considerations on power conversion for electric and plug-in hybrid electric vehicle battery charging in photovoltaic installations. *IEEE transactions on power electronics*, 28(12), 5784-5792.

- Ingersoll, J.G., & Perkins, C.A. (1996, May). The 2.1 kWp photovoltaic electric vehicle charging station in the city of Santa Monica, California. In Conference Record of the Twenty-Fifth IEEE Photovoltaic Specialists Conference-1996 (pp. 1509-1512). IEEE.
- Bai, S., Yu, D., & Lukic, S. (2010, September). Optimum design of an EV/PHEV charging station with DC bus and storage system. In 2010 IEEE Energy Conversion Congress and Exposition (pp. 1178-1184). IEEE.
- Ninad, N.A., & Lopes, L.A. (2007, October). Operation of single-phase grid-connected inverters with large DC bus voltage ripple. In 2007 IEEE Canada Electrical Power Conference (pp. 172-176). IEEE.
- Araújo, S.V., Zacharias, P., & Mallwitz, R. (2009). Highly efficient single-phase transformerless inverters for grid-connected photovoltaic systems. *IEEE Transactions on Industrial Electronics*, 57(9), 3118-3128.
- Meneses, D., Blaabjerg, F., Garcia, O., & Cobos, J.A. (2012). Review and comparison of step-up transformerless topologies for photovoltaic AC-module application. *IEEE Transactions on Power Electronics*, 28(6), 2649-2663.
- D. Meneses, F. Blaabjerg, O. García, and J. A. Cobos, —Review and comparison of step-up transformerless topologies for photovoltaic module application, *IEEE Trans. Power Electron.*, vol. 28, no. 6, pp. 2649–2663, Jun. 2013.
- González, R., Lopez, J., Sanchis, P., & Marroyo, L. (2007). Transformerless inverter for single-phase photovoltaic systems. *IEEE Transactions on Power Electronics*, 22(2), 693-697.
- Kjaer, S.B., Pedersen, J.K., & Blaabjerg, F. (2005). A review of single-phase grid-connected inverters for photovoltaic modules. *IEEE transactions on industry applications*, 41(5), 1292-1306.